Wear 272 (2011) 176–183

Contents lists available at ScienceDirect

Wear

journal homepage: www.elsevier.com/locate/wear

Pattern abrasion of ultra-high molecular weight polyethylene: Microstructure reconstruction of worn surface

Jianzhang Wang[a,*], Beibei Chen[a,b], Fengyuan Yan[a], Qunji Xue[a], Fei Zhao[a]

[a] State Key Laboratory of Solid Lubrication, Lanzhou Institute of Chemical Physics, Chinese Academy of Sciences, Lanzhou 730000, PR China
[b] Graduate University, Chinese Academy of Sciences, Beijing 100049, PR China

ARTICLE INFO

Article history:
Received 5 January 2011
Received in revised form 23 June 2011
Accepted 8 August 2011
Available online 12 August 2011

Keywords:
UHMWPE
NaCl solution
Lubrication
Pattern abrasion
Microstructure reconstruction
Wear resistance

ABSTRACT

The friction and wear behavior of ultra-high molecular weight polyethylene (UHMWPE) sliding against bearing steel (AISI 52100) in a ring-on-block contact mode under the lubrication of aqueous solution of 3.5% NaCl was evaluated. The worn polymer surfaces were analyzed by means of three dimensional profiling, atomic force microscopy, Polarized Raman microanalysis, field emission scanning electron microscopy, and nanoindentation testing. It was found that unusual wavelike abrasion patterns were formed on the worn surface of UHMWPE under properly selected sliding conditions. In the presence of plowing effect, the molecular chains of UHMWPE and short-rod like microcrystalline grains of abrasion pattern were both further oriented along the plowing direction and became tiny and dense owing to microstructure reconstruction. Resultant microstructurally reconstructed worn surface of UHMWPE had a higher nanoindentation hardness and modulus as well as increased wear resistance.

1. Introduction

In general, when a polymer is rubbed, its worn surface will exhibit random wear tracks such as furrows, scratches, cracks or plastic deformation. Surprisingly, on the worn surfaces of rubber, a series of periodic parallel wear tracks is often formed and makes up a pattern, which is called abrasion pattern [1–4]. Abrasion pattern consists of saw-tooth ridges perpendicular to the sliding direction [1,2]. Pattern abrasion as a typical wear mechanism of rubber has been extensively investigated, and many mechanisms such as Schallamatch detached wave theory, stick-slip dynamics, fracture mechanism, and erosion–diffusion process have been proposed to illustrate the formation of abrasion patterns on the worn surfaces of rubber [5].

However, abrasion patterns are rarely observed on the worn surfaces of plastic. Several researchers observed regular scratched patterns on the scratched surfaces of polyolefin plastics [6–10], and they suggested that the zig–zag and quasi-periodic parabolic patterns on the scratched surfaces of polypropylene and polyethylene were attributed to the sequential accumulation and release of tangential force along the moving direction of indenter [6,10]. Recently, we found regular wavelike patterns on the worn surfaces of ultra-high molecular weight polyethylene (UHMWPE) sliding against bearing steel under the lubrication of seawater and aqueous solution of 3.5 wt.% NaCl [11], which is different from the case under dry sliding or pure water lubrication. We considered that the unusual waves normal to the sliding direction were a special plastic deformation of UHMWPE caused by the large plowing effect of hard micro-asperities on the corroded counterface, and a microscopic stick-slip dynamical mechanism could be cited to illustrate the pattern abrasion process of UHMWPE [11]. In that research, nevertheless, little attention was paid to associating the particular abrasion mechanism with the microstructure of polymer. In this article, therefore, the unusual pattern abrasion of UHMWPE plastic under the lubrication of aqueous solution of NaCl is highlighted in relation to the microstructure transformation of UHMWPE.

2. Experimental

2.1. Materials and specimen

UHMWPE powders with an average particle size of 60 μm, a molecular weight of 3×10^6 and a density of 0.935 g/cm^3 were provided by Beijing No. 2 Auxiliary Agent Plant (Beijing, China). The powders were hot-pressed at 3–15 MPa and sintered at 165 °C in a mould, followed by cooling and mould-releasing to generate desired UHMWPE specimens. The crystallinity of the sintered UHMWPE specimens is about 40–50% (determined by differential scanning calorimetry); and their Shore hardness is about 65.

* Corresponding author. Tel.: +86 931 4968078; fax: +86 931 827 7088.
E-mail address: wjzsci@yahoo.cn (J. Wang).

0043-1648/$ – see front matter © 2011 Elsevier B.V. All rights reserved.
doi:10.1016/j.wear.2011.08.014

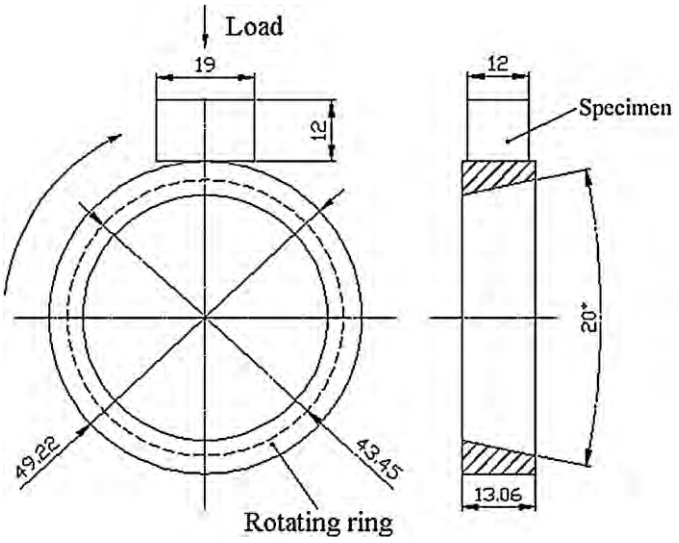

Fig. 1. Schematic contact diagram of the frictional couple (unit: mm).

2.2. Friction and wear test

The friction and wear behavior of UHMWPE were evaluated using a ring-on-block tribology test apparatus (MRH-03 model, Jinan Testing Machine Factory, China). The schematic contact diagram of the frictional couple is shown in Fig. 1. The lower bearing steel (AISI 52100) ring with a size of Φ 49.22 mm × 13.06 mm was driven to rotate against the stationary upper UHMWPE block with a size of 19 mm × 12 mm × 12 mm at a linear velocity of 0.5 m/s, 1.0 m/s and 1.5 m/s, load of 100 N and 200 N, and duration of 120 min. The rubbed surfaces of UHMWPE specimen were perpendicular to the direction of mould pressing. Prior to each test, the rubbed surface of the steel ring was abraded with fine emery paper to a surface roughness of about Ra = 0.10 μm; then the ring and block were ultrasonically cleaned with acetone. The aqueous solution of 3.5 wt.% NaCl with a pH value of 8.2 was used as the lubricating medium, and it was continuously dropped onto the sliding surfaces at a rate of 100–105 drops per minute (300–315 ml per hour) to realize lubrication between the sliding surfaces.

2.3. Observation on the morphologies of worn surfaces

The morphologies of the worn surfaces were examined using a JEM-5600LV scanning electron microscope (SEM) and a MicroXAM three dimensional (3D) surface profiler. In order to increase the resolution of SEM observation, the polymer samples were plated with gold coating to render them electrical conductivity. The fine abrasion pattern of UHMWPE was examined using a CSPM 4000 atomic force microscope (AFM).

2.4. Polarized Raman microanalysis

Polarized Raman scattering spectrometry is powerful in evaluating the molecular chain orientation of semi-crystalline polymers [12–15]. In this study, the method given by Pigeon [12] while investigating the drawing orientation of polyethylene was adopted to evaluate the molecular chain orientation of the abrasion pattern of UHMWPE. The polarized backscattering Raman microanalysis was conducted on the ridges of abrasion pattern and the initial surface of UHMWPE, respectively, with the polarization directions of the incident light and scattered light both parallel to the direction of plowing effect applied to the ridges. The Raman spectra were recorded with a Jobin-Yvon HR800 spectrometer using a Quantum semiconductor laser tuned at 532 nm with a laser power of 1 mW, an integration time of 80 s and a laser spot diameter of 1 μm.

2.5. Permanganic etching and field emission scanning electron microscopic observation

Permanganic etching is an effective technique to uncover the microstructure of melt-crystallized polyolefin [16–18]. In this study, the abrasion pattern and initial surface of UHMWPE were etched using a concentrated sulfuric acid containing 0.8% $KMnO_4$ (volume fraction) to preferentially remove amorphous phases from the etched area and leave intact crystalline region therein. Thus a small rectangular block with a size of 5 mm × 5 mm × 3 mm was cut off from the abrasion pattern or the initial surface of UHMWPE and ultrasonically etched in 10 ml of the etching reagent for 12 min. The etching process was conducted for only 12 min so that the wavelike pattern roughly remained intact after being etched. After the etched surfaces were sequentially treated in the manners reported elsewhere [18], resultant etched surfaces were observed using a Hitachis-4800 field emission scanning electron microscope (FESEM).

2.6. Nanoindentation test

The nanomechanical properties of the ridges of abrasion pattern and the initial surface of UHMWPE were examined using a nanoindenter (Nanotest 600, Micro Materials Ltd., MML) fitted with a three-sided pyramidal Berkovich diamond indenter which was with a radius of 200 nm, an elastic modulus of 1141 GPa and a Poisson's ratio of 0.07. The indenter was driven into the surface at a constant loading rate of 30 μN/s until an indentation depth of 1200 nm was reached. After held for 5 s, the indenter was unloaded

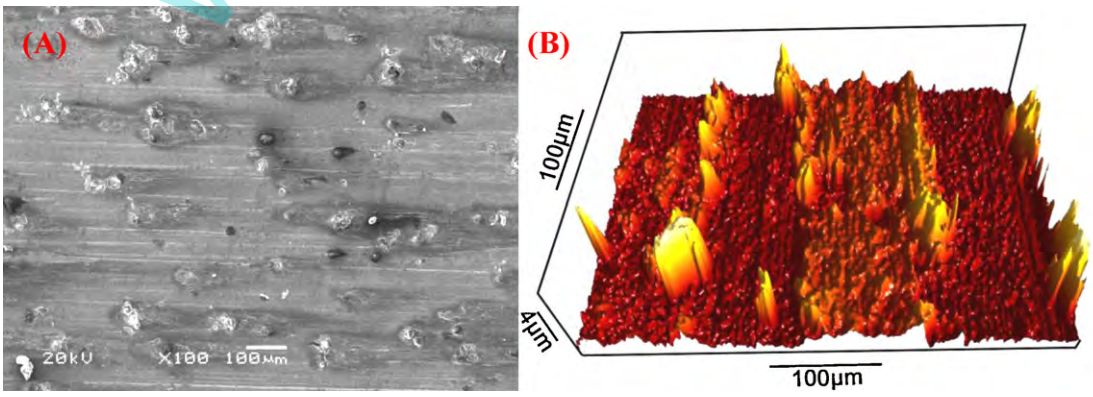

Fig. 2. SEM image (A) and 3D profile (B) of corroded counterface under lubrication of NaCl solution.

Table 1
Relationship between the topography of counterface and the formation of abrasion pattern.

Sliding conditions	Increase in surface roughness of counterface/μm[a]	Friction force/N	Wave-length/μm	Wave-height/nm
1.5 m/s, 100 N	0.1	2.75	–[b]	–
1.0 m/s, 100 N	0.3	7.51	6	100–450
0.5 m/s, 100 N	1.1	16.6	13	400–750
0.5 m/s, 200 N	1.7	30.3	25	1000–1600
0.5 m/s, 300 N	1.8	45.1	–	–

[a] The initial surface roughness of counterface is about 0.1 μm.
[b] The symbol "–" shows that no abrasion pattern is formed on the worn surface of UHMWPE.

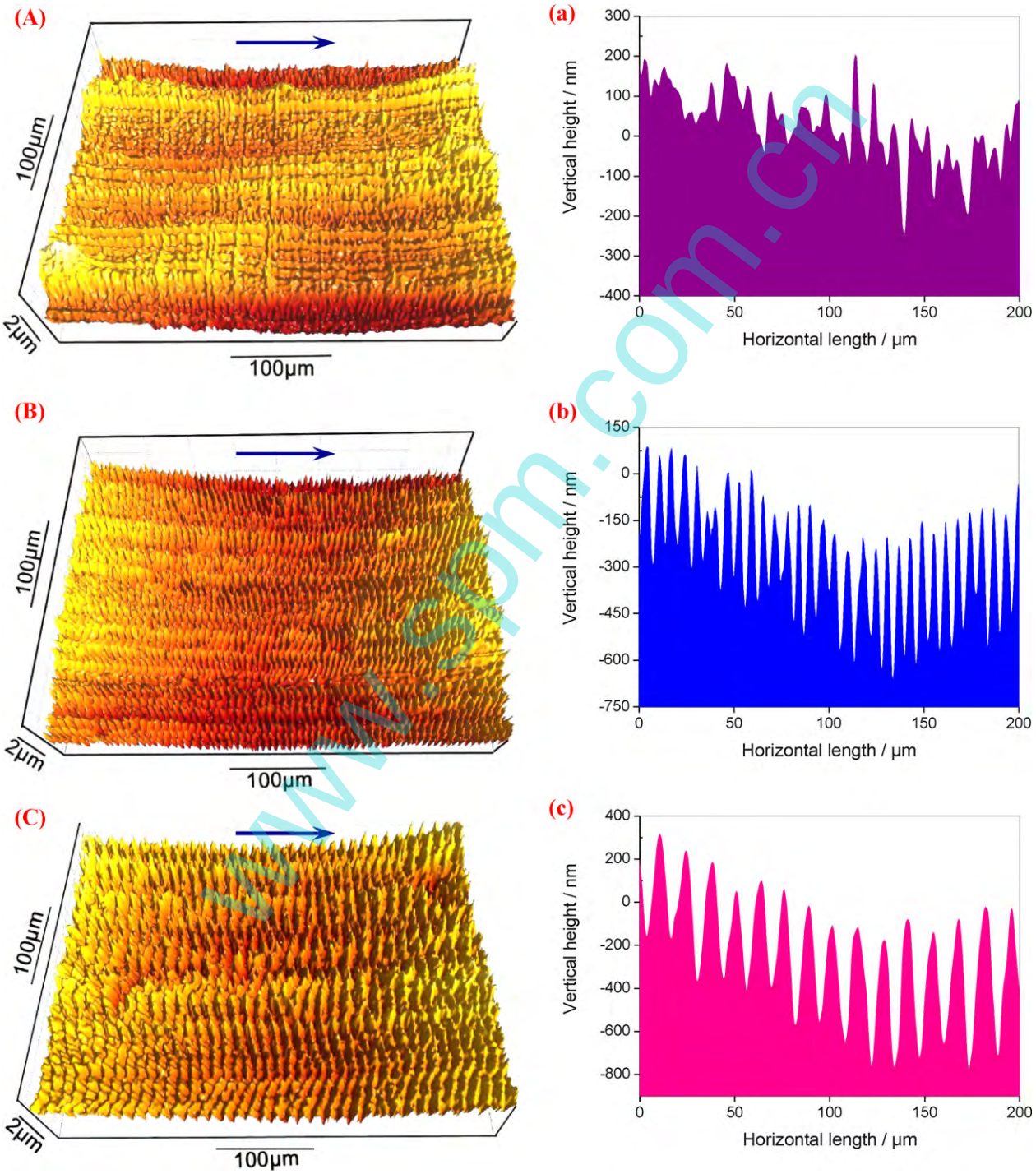

Fig. 3. 3D profiles (A)–(E) and cross sections (a)–(e) along the sliding direction of worn surfaces of UHMWPE against GCr15 under different sliding conditions. (A) plus (a): 1.5 m/s and 100 N; (B) plus (b): 1.0 m/s and 100 N; (C) plus (c): 0.5 m/s and 100 N; (D) plus (d): 0.5 m/s and 200 N; and (E) plus (e): 0.5 m/s and 300 N. The arrows indicate the sliding direction, i.e., the direction of plowing effect.

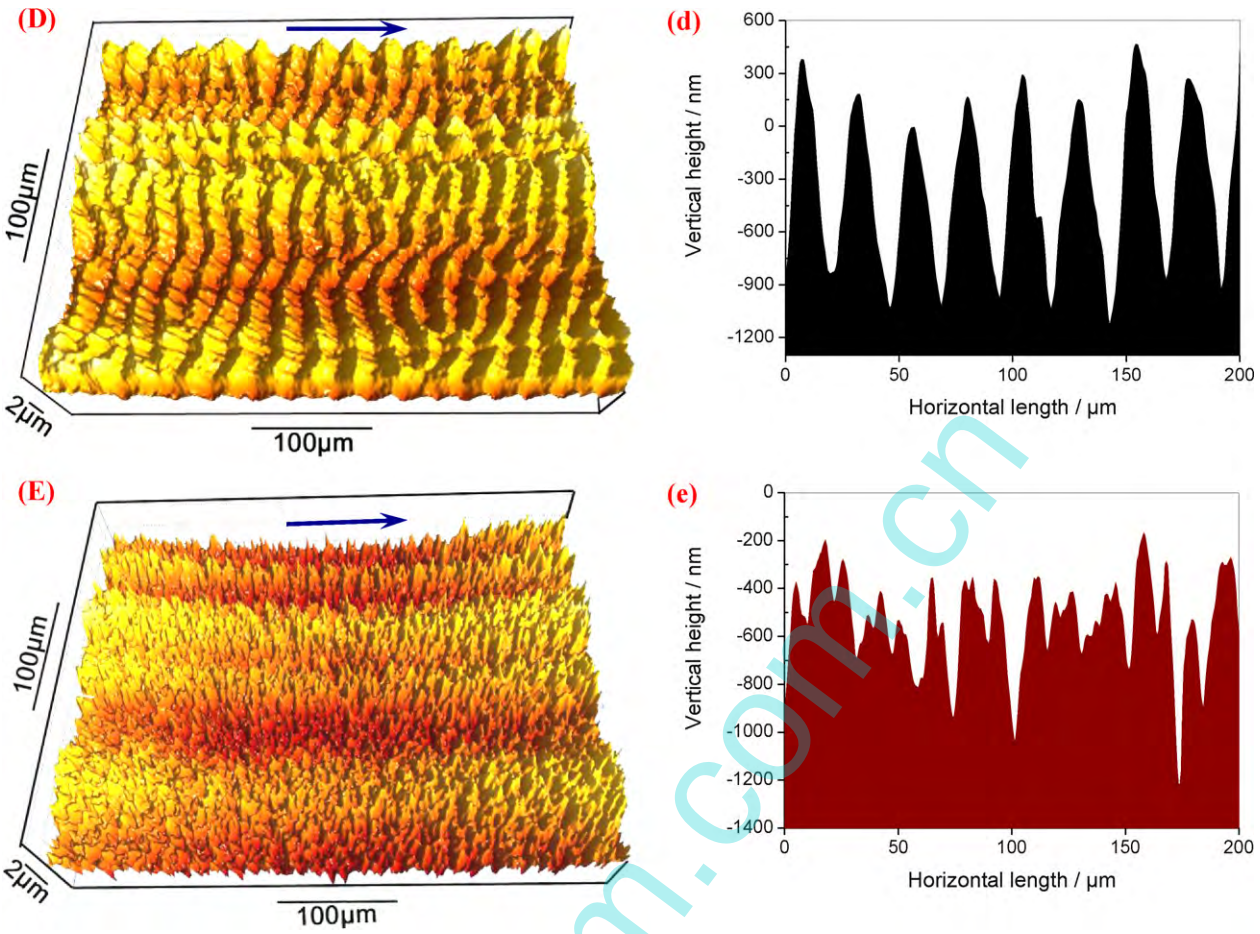

Fig. 3. (*Continued.*)

at a rate of 30 μN/s. For each specimen, five indentations were made at different sections. A Poisson's ratio 0.36 of UHMWPE was used to calculate the elastic modulus [19].

Surface roughness plays an important role in the determination of mechanical properties from nanoindentation tests, especially at low indentation depth. It can cause an uncertainty in contact area due to asperity contact at very shallow indentation depths. According to the standard of ISO 14577, to maintain the contribution of surface roughness to the uncertainty in indentation depth below 5%, the indentation depth h shall be at least 20 × the arithmetic mean deviation roughness Ra, namely $h \geq 20\ Ra$. Therefore, prior to indentation test the initial surface of UHMWPE was polished carefully with 1 μm alumina powder to a Ra surface roughness about 40 nm. The surface roughness was estimated by a CSPM 4000 atomic force microscope (AFM).

3. Results and discussion

3.1. Formation and morphology of abrasion pattern

Our previous study suggests that the wavelike abrasion pattern of UHMWPE is a kind of special plastic deformation of worn surface associated with the large plowing effect of hard asperities on counterface [11]. Under the lubrication of aqueous solution of NaCl, pitting corrosion occurred on steel counterface, as a result, micro-asperities were formed on the counterface in association with the accumulation of corrosive products and roughening of the counterface (see Fig. 2). It should be noted that under different sliding conditions, namely different velocities and loads, the corroded extent of the steel counterface is different, corresponding to different extent of increase of the counterface surface roughness (see Table 1). Along with the formation of micro-asperities, the plowing suffered by polymer surface is enhanced, resulting in increased friction force and friction heat of the sliding couples. In the meantime, UHMWPE possessing poor heat resistance is easily softened and plastically deformed in the presence of plentiful friction heat, promoting pattern abrasion. However, the adhesion between the frictional surfaces will be significantly enhanced owing to the softening of the rubbed surface of UHMWPE, thereby destroying the regular abrasion pattern. Therefore, it can be supposed that the formation of abrasion pattern on the rubbed surface of UHMWPE is attributed to the compromise between plowing effect and adhesion effect under lubricated conditions.

Fig. 3 shows the 3D morphology and cross-section of worn surfaces of UHMWPE under different sliding conditions. And Fig. 4 shows the scanning electron micrographs of the worn surfaces. It can be seen that the formation of abrasion pattern is closely related to the sliding conditions, in particular, to the topography of counterface. Under a high sliding velocity of 1.5 m/s and low load of 100 N, the counterface is slightly roughened, corresponding to very weak plowing effect, very low friction force and friction heat, and consequent very weak plastic deformation of UHMWPE. As a result, the worn surface of UHMWPE in this case is smooth and shows no abrasion pattern (Figs. 3(A) and 4(A)). When the sliding velocity is decreased to 0.5 m/s and the load increased to 300 N, the counterface is seriously roughened. Subsequently, the plowing effect suffered by UHMWPE is large enough, and so is the friction heat. In

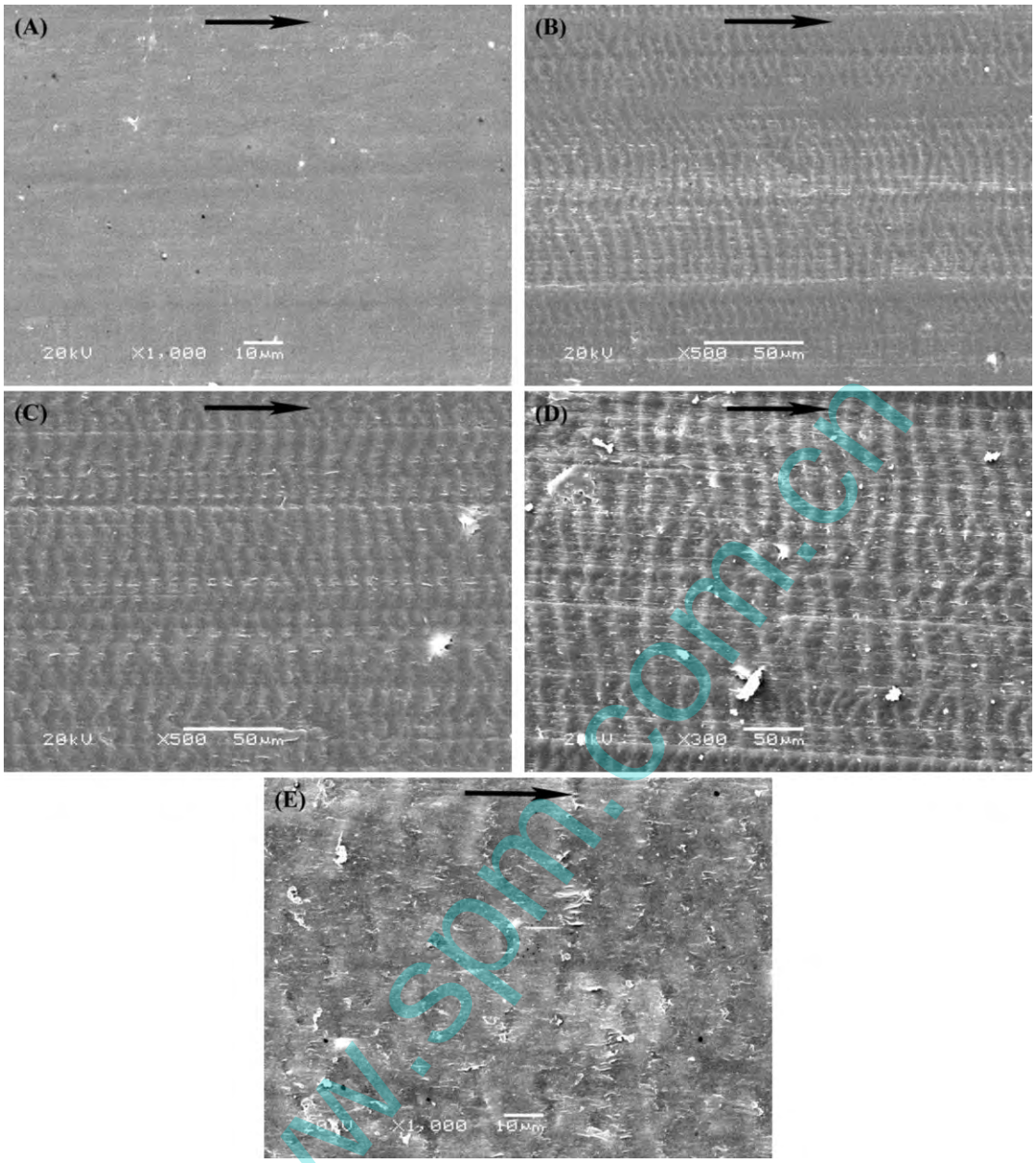

Fig. 4. SEM images of the worn surface of UHMWPE against GCr15 under different sliding conditions. (A) 1.5 m/s and 100 N; (B) 1.0 m/s and 100 N; (C) 0.5 m/s and 100 N; (D) 0.5 m/s and 200 N; and (E) 0.5 m/s and 300 N. The arrows indicate the sliding direction.

this case, the effect of friction heat cannot be fully set off by the cooling effect of the lubrication medium. As a result, the worn surface of UHMWPE is dominated by softening adhesion but shows no regular abrasion pattern (Figs. 3 and 4(E)). Only under favored sliding conditions (0.5 m/s and 100 N; 0.5 m/s and 200 N; 1.0 m/s and 100 N), the counterface is roughened to a desired extent, thereby leading to regular wavelike patterns on the worn surface of UHMWPE (Figs. 3 and 4(B)–(D)). In these cases, the plowing effect is large enough to cause sufficient plastic deformation of UHMWPE but not to bring too much frictional heat resulting in softening adhesion of the worn surface. Therefore, as mentioned earlier, the formation of abrasion pattern on the worn surface of UHMWPE is a result of competition equilibrium between plowing effect and adhesion effect suffered by rubbed UHMWPE surface. In addition, both the wave-length (the average distance between adjacent ridges) and wave-height (the height of ridges) of wavelike pattern grow with the increase of surface roughness of the counterface.

Fig. 5 shows the fine 3D structures of the abrasion pattern (AFM images). It can be seen that the abrasion pattern of UHMWPE consists of a series of parallel ridges perpendicular to the sliding direction, and many fine furrows exist along the sliding direction. This once again indicates that the plowing effect is the external driving force to facilitate the formation of the abrasion pattern.

3.2. Molecular orientation of abrasion pattern

When a linear macromolecule is stretched sufficiently, its length can be several hundreds or thousands, even tens of thousands times as much as its width. Such uneven asymmetry of configuration makes the macromolecules easily parallel arrange predominately along a particular direction in some situations such as under the effect of force field, which is the so-called orientation. The orientation of polymer involves the preferential arrangement of macromolecular chains, chain segments, crystal chips and zones.

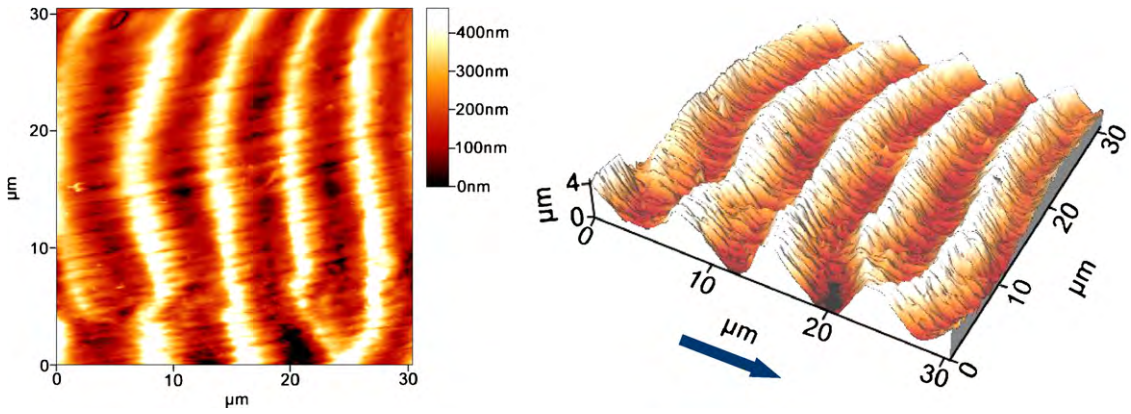

Fig. 5. AFM images of the worn surface of UHMWPE sliding under 1.0 m/s and 100 N. The arrow indicates the sliding direction.

Owing to the orientation, the mechanical properties of polymer materials along the direction of orientation can be enhanced greatly.

An effective method proposed by Pigeon [12] while investigating the drawing orientation of polyethylene was adopted to evaluate the molecular chain orientation of UHMWPE. According to the method, when the polarization directions of the incident light and scattered light were both parallel to the draw direction, the backscattering Raman spectrum of polyethylene in the C–C stretching mode region was quite sensitive to the orientation of polyethylene chains. In the Raman spectrum, the feature at 1130 cm^{-1} was assigned to symmetric C–C stretching mode of the all-trans conformation associated with both crystalline and amorphous phases, whether the feature at 1060 cm^{-1} was assigned to C–C anti-symmetric stretching mode associated with both crystalline and amorphous phases [12,13]. There was a fairly good correlation between the peak height intensity ratio h_{1130}/h_{1060} and the orientation coefficients, that is, the larger the value of h_{1130}/h_{1060}, the larger the orientation coefficient of molecular chain, accordingly the higher the chain orientation [12]. In this way, the distribution of oriented C–C bonds with trans conformation in polyethylene can be readily determined by measuring the peak height intensity ratio h_{1130}/h_{1060} in backscattering polarized Raman spectrum while adjusting the polarization directions of the incident light and scattered light parallel to the direction of external force.

Fig. 6 shows the C–C stretching mode regions of the backscattering polarized Raman spectra of abrasion pattern and the initial surface of UHMWPE, with the polarization directions of the incident light and scattered light both parallel to the direction of plowing effect applied on the ridges. As can be seen, the abrasion pattern has a larger peak height intensity ratio (h_{1130}/h_{1060}, the height ratio of the peaks at 1130 cm^{-1} and 1060 cm^{-1}) as compared with the initial surface, and the value of h_{1130}/h_{1060} rises with increasing plowing effect. Interestingly, the initial surface of UHMWPE has an h_{1130}/h_{1060} value of 1.7 but not 1.0 indicating no orientation [12]. This suggests that the molecular chains of the initial surface (the mould-pressed surface) of UHMWPE are originally oriented to some extent along the sliding direction (the direction perpendicular to the mould pressing), the same as that reported elsewhere [20]. Since the peak height intensity ratio h_{1130}/h_{1060} is well correlated with the orientation coefficients, and a larger value of h_{1130}/h_{1060} corresponds to a bigger orientation coefficient as well as a higher content of oriented C–C bonds with trans conformation [12], the molecular chains of the abrasion pattern tend to further orient along the direction of plowing effect as compared with that of the initial surface, and a large plowing effect causes a more remarkable orientation.

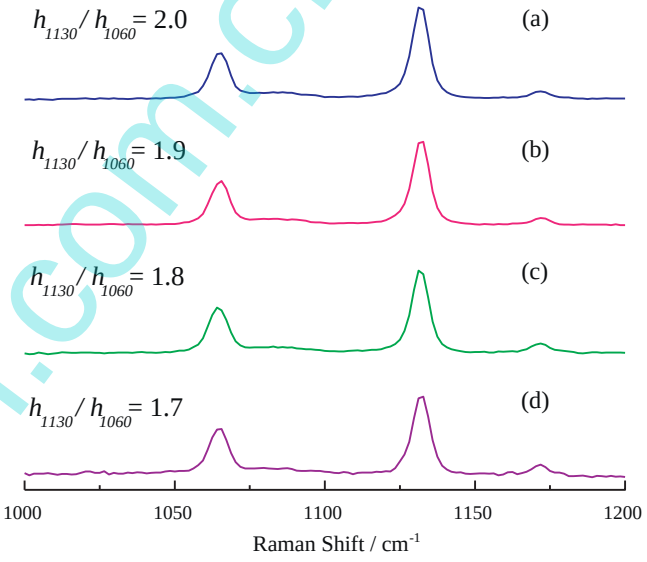

Fig. 6. Backscattering Raman analysis on the ridges of abrasion patterns and the initial surface of UHMWPE. (a) abrasion pattern formed under 0.5 m/s and 200 N; (b) abrasion pattern formed under 0.5 m/s and 100 N; (c) abrasion pattern formed under 1.0 m/s and 100 N; and (d) the initial surface.

3.3. Microcrystalline morphology of abrasion pattern

As stated above, the molecular chains of the abrasion pattern of UHMWPE are oriented under plowing effect, which involves the chains in both amorphous phase and crystalline phase. Thus, it can be inferred that the microcrystalline morphology of the abrasion pattern may also be transformed to some extent as compared with that of the initial surface. To directly reflect such a transformation, we treated the abrasion pattern using permanganic etching with which the amorphous region was preferentially etched away and the crystalline region was kept almost intact. Fig. 7 shows the FESEM images of the etched initial surface and abrasion patterns of UHMWPE. Interestingly, the mould-pressed microcrystals of UHMWPE have a short-rod shape but not appear as commonly observed microchips or spherulites. The rod-like microcrystals with a diameter of about 100 nm and non-uniform length are initially oriented to some extent along the sliding direction, highly consistent with the results of polarized Raman analysis (Fig. 7(A)). Moreover, the crystalline morphology of the abrasion pattern of UHMWPE is somewhat different from that of the initial surface. Namely, the microcrystalline in the abrasion pattern of UHMWPE tends to orient more strongly than that of the initial surface; and

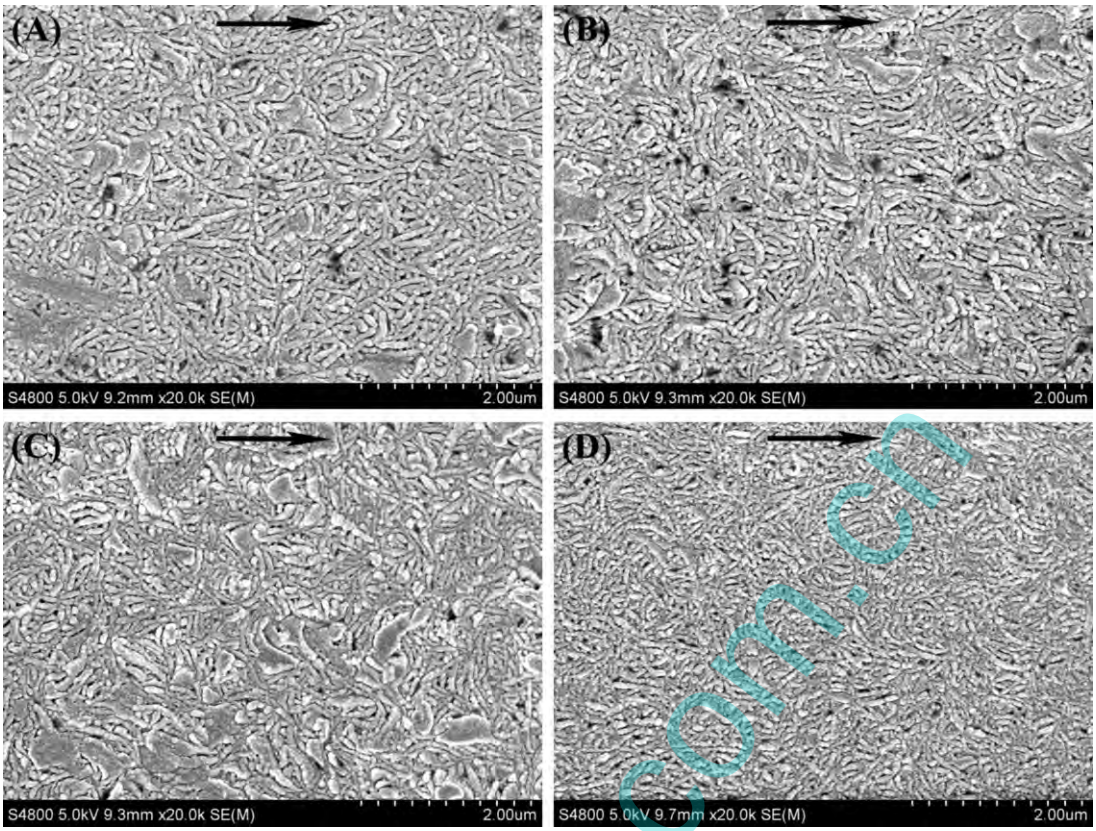

Fig. 7. FESEM images of etched initial surface and abrasion patterns of UHMWPE formed under different sliding conditions. (A) initial surface; (B) abrasion pattern formed under 1.0 m/s and 100 N; (C) abrasion pattern formed under 0.5 m/s and 100 N; and (D) abrasion pattern formed under 0.5 m/s and 200 N. The arrows indicate the sliding direction.

the microcrystal grains of the abrasion pattern are more tiny and dense than the rod-like microcrystalline grains of the initial surface. And interestingly, with increasing plowing effect and consequent friction heat, the extent of orientation, refinement and compacting of microcrystalline grains of the abrasion patterns are gradually increased (Fig. 7(B)–(D)). In combination with polarized Raman microanalysis, it can be concluded that under the plowing effect of the asperities on counterface, the microstructure of the worn surface of UHMWPE is reconstructed, resulting in regular wavelike abrasion pattern. This inelastic response of the microstructure of UHMWPE may begin with molecular plastic flow in the amorphous regions via inter-microcrystal shear, inter-microcrystal separation and microcrystal-stack rotation under the plowing effect and consequent friction-heat effect, resulting in the formation of the abrasion ridges before the passing asperities of the counterface [11,21]. Either tied or entangled molecular chains would be heavily strained consequently. Once plastic deformation in the amorphous regions is exhausted, the crystalline rods are deformed predominantly through crystallographic slip [21]. As a result, the wavelike abrasion patterns are formed by repeating a stick-slip process [11], in which the rod-like micro-crystals are further oriented to the sliding direction, and become tinier and denser than that of the initial surface of UHMWPE.

3.4. Nanoindentation testing of abrasion pattern

As mentioned above, the microstructure of the abrasion pattern was reconstructed during lubricated sliding. To confirm whether the microstructural reconstruction resulted in change in the micromechanical properties of the abrasion pattern, we conducted nanoindentation analysis on the top of the abrasion ridge and initial surface, respectively. As shown in Fig. 8, the abrasion

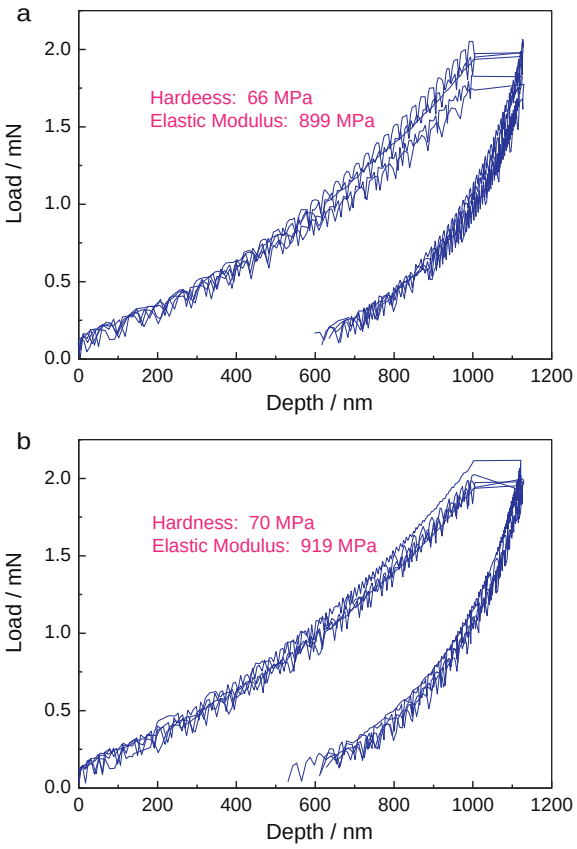

Fig. 8. Nanoindentation curves of the initial surface (A) and the top of abrasion pattern of UHMWPE (B) formed under 0.5 m/s and 200 N.

ridges possess higher nanoindentation hardness and elastic modulus than the initial surface of UHMWPE. This indicates that the abrasion patterning associated with plowing effect does not result in increased wear of polymer as predicted by many researchers [21] but contributes to increase the mechanical strength and wear-resistance of the rubbed surface of UHMWPE to some extent, due to the molecular orientation as well as refinement and compacting of microcrystalline grains. In this way, the flexible UHMWPE molecules adjust their status so as to adapt to destroying from external environment, reducing loss as much as possible, which is a kind of very "smart" transformation of microstructure. Such a phenomenon is often observed in nature when something prevents itself from the eroding of external force by accumulating its micro-constructional units to form a wavelike pattern. For instance, after a strong wind, the sand grains in desert often takes on a very regular wavelike accumulation; and after a flood the soil of the riverbed also presents a wavelike accumulation. The commonness of such macroscopic and microscopic patterning transformations is the flowing and accumulation of microstructure units of materials or things. Under external forces, a large number of microstructure units of materials flow along the direction of force and then accumulate, resulting in the enhancement of material strength and resistance to external force.

4. Conclusions

1. Under the plowing effect, the molecular chains and short-rod like microcrystalline grains of abrasion pattern are both further oriented along the plowing direction as compared with that of the initial surface of UHMWPE, resulting in wavelike abrasion pattern of UHMWPE owing to the competition equilibrium between the plowing effect and adhesive effect suffered by the worn surface.
2. Due to the microstructure reconstruction of worn surface associated with the formation of abrasion pattern under plowing effect, the grains of the abrasion pattern become tiny and dense than that of the initial surface, resulting in increased nanoindentation hardness and modulus as well as wear-resistance of UHMWPE.

Acknowledgements

The research is financially supported by National Natural Science Foundation of China (Grant No. 50823008) and National High-Tech Research and Development Program of China ("863" Program, grant No. 2009AA03Z105).

References

[1] Y. Uchiyama, Y. Ishino, Pattern abrasion mechanism of rubber, Wear 158 (1992) 141–153.
[2] T. Iwai, Y. Uchiyama, K. Shimosaka, K. Takase, Study on the formation of periodic ridges on the rubber surface by friction and wear monitoring, Wear 259 (2005) 669–675.
[3] A. Schallamach, How does rubber slide, Wear 17 (1971) 301–312.
[4] M. Barquins, Friction and wear of rubber-like materials, Wear 160 (1993) 1–11.
[5] M.D. Acunto, S. Napolitano, P. Pingue, P. Giusti, P. Rolla, Fast formation of ripples induced by AFM: a new method for patterning polymers on nanoscale, Mater. Lett. 61 (2007) 3305–3309.
[6] A. Dasari, J. Rohrmann, R.D.K. Misra, Atomic force microscopy assessment of mechanically induced scratch damage in polypropylenes and ethylene–propylene di-block copolymers, Mater. Sci. Eng. A 354 (2003) 67–81.
[7] A. Dasari, J. Rohrmann, R.D.K. Misra, Atomic force microscopy characterisation of mechanically induced surface damage in ethylene–propylene diblock copolymeric materials, Mater. Sci. Technol. 19 (2003) 1458–1466.
[8] A. Dasari, J. Rohrmann, R.D.K. Misra, Atomic force microscopy characterisation of scratch deformation in long and short chain isotactic polypropylenes and ethylene–propylene copolymers, Mater. Sci. Technol. 19 (2003) 1298–1308.
[9] A. Dasari, J. Rohrmann, R.D.K. Misra, On the scratch deformation of micrometric wollastonite reinforced polypropylene composites, Mater. Sci. Eng. A 364 (2004) 357–369.
[10] Q. Yuan, N. Ramisetti, R.D.K. Misra, Nanoscale near-surface deformation in polymer nanocomposites, Acta Mater. 56 (2008) 2089–2100.
[11] J.Z. Wang, F.Y. Yan, Q.J. Xue, Friction and wear behavior of ultra-high molecular weight polyethylene sliding against GCr15 steel and electroless Ni-P alloy coating under the lubrication of seawater, Tribol. Lett. 35 (2009) 85–95.
[12] M. Pigeon, R.E. Prud'homme, M. Pézolet, Characterization of molecular orientation in polyethylene by Raman spectroscopy, Macromolecules 24 (1991) 5687–5694.
[13] M.J. Citra, D.B. Chase, R.M. Ikeda, K.H. Gardner, Molecular orientation of high-density polyethylene fibers characterized by polarized Raman spectroscopy, Macromolecules 28 (1995) 4007–4012.
[14] G.A. Voyiatzis, K.S. Andrikopoulos, G.N. Papatheodorou, E.I. Kamitsos, G.D. Chryssikos, J.A. Kapoutsis, S.H. Anastasiadis, G. Fytas, Polarized resonance Raman and FTIR reflectance spectroscopic investigation of the molecular orientation in industrial poly(vinylchloride) specimens, Macromolecules 33 (2000) 5613–5623.
[15] L. Lauchlan, J.F. Rabolt, Polarized Raman measurements of structural anisotropy in uniaxially oriented Poly(vinylidene fluoride) (Form I), Macromolecules 19 (1986) 1049–1054.
[16] R.H. Olley, D.C. Bassett, An improved permanganic etchant for polyfines, Polymer 23 (1982) 1707–1710.
[17] M.M. Shahin, R.H. Olley, M.J. Blissett, Refinement of etching techniques to reveal lamellar profiles in Polyethylene banded spherulites, J. Polym. Sci. Polym. Phys. 37 (1999) 2279–2286.
[18] K.L. Naylor, P.J. Philips, Optimization of permanganic etching of Polyethylene for scanning electron microscopy, J. Polym. Sci. Polym. Phys. 21 (1983) 2011–2026.
[19] K.S.K. Karuppiah, A.L. Bruck, S. Sundararajan, J. Wang, Z.Q. Lin, Z.H. Xu, X.D. Li, Friction and wear behavior of ultra-high molecular weight polyethylene as a function of polymer crystallinity, Acta Biomater. 4 (2008) 1401–1410.
[20] A. Bellare, R.E. Cohen, Morphology of rod stock and compression-moulded sheets of ultra-high-molecular-weight polyethylene used in orthopaedic implants, Biomaterials 17 (1996) 2325–2333.
[21] W. Shi, H. Dong, T. Bell, Tribological behaviour and microscopic wear mechanisms of UHMWPE sliding against thermal oxidation-treated Ti6Al4V, Mater. Sci. Eng. A 291 (2000) 27–36.